Dry-etch of As_2S_3 thin films for optical waveguide fabrication

Weitang Li,[a] Yinlan Ruan, Barry Luther-Davies, and Andrei Rode
Laser Physics Center, The Australian National University, Canberra 0200, Australia

Rod Boswell
Plasma Research Lab, The Australian National University, Canberra 0200, Australia

(Received 9 June 2005; accepted 1 August 2005; published 24 October 2005)

Plasma etching to As_2S_3 thin films for optical waveguide fabrication has been studied using a helicon plasma etcher. The etching effects using the processing gases or gas mixtures of O_2, Ar, and CF_4 were compared. It was found that the O_2 plasma had no chemical etching effect to the As_2S_3, but it could oxidize the surface of the As_2S_3. The Ar plasma provided a strong ion sputtering effect to the films. The CF_4 plasma exhibited a too strong chemical etch to the As_2S_3, leading to serious undercutting and very rough sidewalls of the waveguides. Ar and O_2 gases were compared as the additives to dilute the CF_4 processing gas. The etch rate of the As_2S_3 was reduced dramatically from over 2000 nm/min to a few hundred nm/min when the pure CF_4 gas was heavily diluted with 70% Ar or O_2 gas. The undercutting and sidewall roughness of the etched waveguides were also decreased greatly when above dilution was made, which was associated with an enormous weakening of the isotropic chemical etch induced by neutral reactants in the plasma. In addition, the O_2 showed a better dilution effect than the Ar in reducing the etch rate of the As_2S_3; and the O_2/CF_4 plasma also enabled a much lower erosion rate to Al mask layers than the Ar/CF_4 plasma at similar plasma conditions. The As_2S_3 waveguides with near vertical and very smooth sidewalls were obtained using an optimized O_2/CF_4 plasma. Moreover, the etching behaviors and mechanisms were explained base on the etching results, and on the characteristics of the applied plasma diagnosed using Langmuir probe and optical spectroscopy techniques. © *2005 American Vacuum Society.* [DOI: 10.1116/1.2049308]

I. INTRODUCTION

Chalcogenide glasses possess third order optical nonlinearities more than 500 times higher than fused silica, with similar response times and favorable nonlinear figure of merit. They, therefore, can be used for fast all-optical processing, including all-optical multiplexing and demultiplexing; wavelength conversion; Raman and parametric amplification.[1–3] Chalcogenides form glasses over a wide range of compositions, allowing their refractive indexes to be tuned to obtain very high index contrast between the core and cladding of a waveguide. This makes single mode waveguides with small cross-sectional area and small bend radii achievable. As a result, low peak power (<1 W) all-optical processing is possible in planar waveguide structures fabricated in chalcogenide glasses. In addition, chalcogenides are also promising for magneto-optic devices, due to their moderate Verdet constants in the infrared.[3]

To realize their potential applications, the chalcogenides, need to be patterned into micro-sized low loss optical waveguides. Techniques for producing high-quality chalcogenide glass films, including thermal evaporation, sputtering, chemical vapor deposition, and pulsed laser deposition, have been well developed.[4–6] However, patterning the chalcogenide films into waveguides remains a difficulty. Laser-writing has been used to generate waveguides using the well-known photosensitivity of chalcogenides to light near their band edge.[5,7] The photo-induced refractive index change is, however, not stable in the long term due to relaxation of the structure, and is, therefore, unsuitable for devices. Wet-etch can also be used, but being an isotropic process serious undercutting of the mask always occurs making the control of waveguide dimensions difficult.[5] Recently, chalcogenide waveguides were fabricated using Ar-plasma etching.[4] The profile of the generated waveguides was, however, not rectangular due to a very poor etching selectivity between the chalcogenide glass and photoresist mask.

In this work, dry etching to As_2S_3 chalcogenide glasses using CF_4-based plasma was studied. It was found that the etch rate of As_2S_3 by pure CF_4 plasma was extremely high, $\sim 1.5-3$ μm/min depending on the plasma power, making the control of the etch depth and waveguide profile very difficult, and thus the CF_4 gas needed to be diluted. O_2 and Ar gases were tested as the additive gases. The etching characteristics using different gases or gas mixtures of O_2, Ar, and CF_4 were investigated and compared for a better understanding of the etching behavior and mechanism.

As_2S_3 waveguides with near vertical and smooth sidewalls were achieved using an optimized CF_4/O_2 plasma. The waveguides were shown to have a low loss of ~ 0.25 dB/cm at 1550 nm, and to be suitable for application in all-optical processing.[8] The waveguide fabrication process is fully compatible with mature silicon microelectronics fabrication methods, and thus is highly suitable for device production.

---

[a] Electronic mail: weitang.li@anu.edu.au

II. EXPERIMENTS

Thin films of the As_2S_3 chalcogenide glasses were deposited on 4-in.-diameter silicon wafers using an ultrafast pulsed laser ablation technique (UFPLA).[9] This technique employs a frequency doubled mode-locked Nd:YAG laser producing 6–7 W average power (70–80 nJ/pulse) at 532 nm, at a repetition rate of 76 MHz. The technique has been proven to produce atomically smooth films free from particle contamination.

Before dry-etching, Al films of 300–400 nm thick were sputter-coated onto the samples and patterned to create etch resistant masks using standard photolithography and wet etching techniques. To prevent the Al films from peeling off during processing due to the mismatch of the thermal expansion coefficients of Al and As_2S_3, a thin (<100 nm) photoresist layer was usually spin-coated onto the As_2S_3 surface prior to sputter-coating the Al mask layer.

Dry etching was carried out in a helicon plasma etcher, which is a high-density low-pressure plasma system.[10] It consists of two joined chambers, the source and diffusion chambers. The source chamber is a 15-cm-diameter, 25-cm-long glass tube surrounded by a "Boswell-type" helicon antenna and two solenoids. The diffusion chamber is a 30-cm-diameter and 30-cm-long aluminum cylinder surrounded by two additional solenoids. The currents in the 4 solenoids are adjusted to produce a magnetic field of 100 G in the source and 60 G in the diffusion chamber. The substrate holder is mounted at the bottom of the diffusion chamber, and is water-cooled. Both the source antenna and the substrate holder are driven by 13.56 MHz rf power sources. The chambers are pumped with an ATP 400 HPC turbomolecular pump. The processing gases (CF_4, O_2, and Ar) are admitted into the vacuum chamber through 3 separate mass flow controllers.

For diagnosing the plasma, a Langmuir probe was used to measure the ion saturation current at the substrate position. A −63 V dc voltage was applied to the probe tip to collect positive ions only. In addition, a *Monolite 6602* optical spectrum analyzer was used to measure the optical emission intensities of fluorine atoms at the wavelength of 684.6 nm. For all these diagnosing measurements, there was no rf power applied to the substrate.

The etch rates of the As_2S_3 and the Al mask were measured *in situ* using an ellipsometer, or *ex situ* using a surface profilometer. The microprofiles of the waveguides were investigated under a field emission scanning electron microscopy (FESEM). The sidewall roughness of the waveguides was determined by measuring the average amplitude of the corrugations or ripples within a 2-μm range on the sidewalls using the FESEM.

III. RESULTS AND DISCUSSIONS

A. Characteristics of the plasma

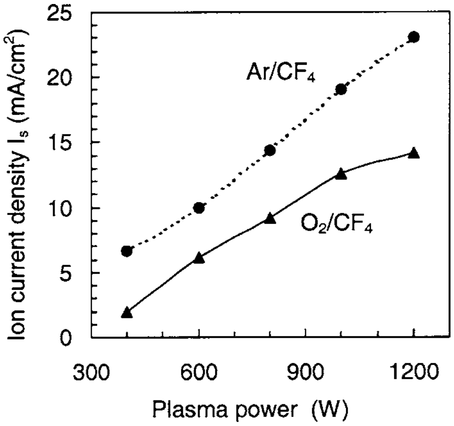

FIG. 1. Ion saturation current at the substrate location vs the plasma power for the gas mixtures of $Ar/CF_4=7/3$ and $O_2/CF_4=7/3$. The pressure was 10 mTorr, and the substrate was not biased.

To understand the plasma-etching behaviors to the As_2S_3 films, the characteristics of the applied plasma were diagnosed using the Langmuir probe and the optical spectroscopy techniques. Figure 1 shows the dependencies of the ion saturation currents (I_s) at the wafer location on the plasma power (P) for the gas mixtures of Ar/CF_4 and O_2/CF_4. The gas flow rates were 70 sccm for both Ar and O_2, and 30 sccm for CF_4, the gas pressure was kept at 10 mTorr, and no substrate rf bias was applied. As seen in Fig. 1, I_s increases almost linearly with P for both the Ar/CF_4 and O_2/CF_4 gas mixtures, indicating the ion and electron densities increase with P. It is also seen in the figure that the I_s of the Ar/CF_4 plasma is obviously much higher than that of the O_2/CF_4 plasma at the same P. This is caused by the fact that Ar gas has much higher ionization efficiency in the plasma than the electronegative O_2 gas.

Figure 2 shows the variations of I_s versus the Ar/CF_4 and O_2/CF_4 gas flow ratios, which were measured at $P=600$ W and pressure 10 mTorr. As shown here, I_s increases slightly, but decreases, with the increase of the Ar/CF_4 or O_2/CF_4 gas flow ratio, respectively.

In addition, the dependence of I_s on the plasma pressure was measured at $P=600$ W for both the gas mixtures of $Ar/CF_4=7/3$ and $O_2/CF_4=7/3$. The results are displayed in Fig. 3. It is seen here that for both the gas mixtures, I_s in-

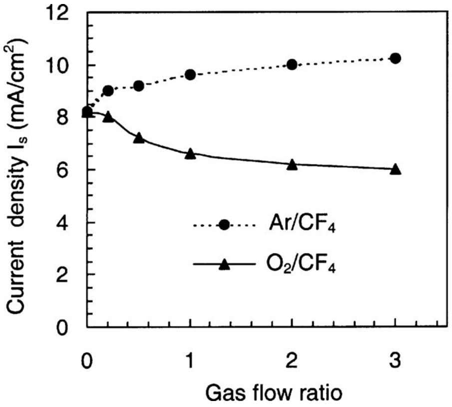

FIG. 2. Ion saturation current vs the gas flow ratio of Ar/CF_4 or O_2/CF_4. The plasma power was 600 W, pressure 10 mTorr, and the substrate was not biased.

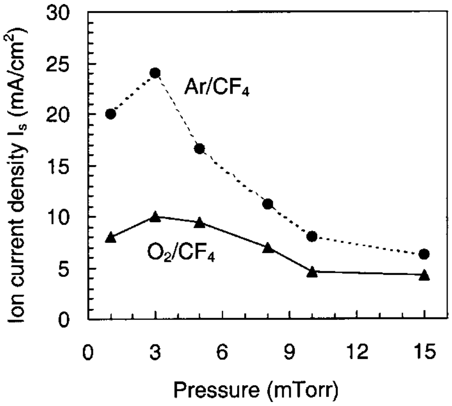

FIG. 3. Variation of the ion saturation current with the plasma pressure for the gas mixture of $Ar/CF_4=7/3$ or $O_2/CF_4=7/3$. The plasma power was 600 W, and the substrate was not biased.

creases when reducing the pressure from 15 to 3 mTorr, reaches a maximum at ~3 mTorr, and then decreases with further reduction of the pressure.

In order to get the information about the concentration of the reactive species in the plasma, the optical emission intensity of the atomic F (I_F) at the wavelength of 684.6 nm was measured. The I_F depends on the concentration of the F atoms dissociated from the CF_4, and on the excitation efficiency of the plasma to the F atoms. Therefore I_F is related to the dissociation ratio of the CF_4 gas, and it also indirectly reflects the density of other species (CF, CF_2, CF_3), since the more F atoms are dissociated from the CF_4, the more other species are generated at the same time.[11] The excitation efficiency is related to plasma density, especially the electron density, since the electrons are the main source to excite the F atoms.

The variation of I_F versus the plasma power P was plotted in Fig. 4. The gas mixtures were also $Ar/CF_4=7/3$ and $O_2/CF_4=7/3$, and the plasma pressure 10 mTorr. As seen in Fig. 4, I_F increases almost linearly with P, and the I_F for the Ar/CF_4 plasma is obviously much higher than that of the O_2/CF_4 plasma at the same P. Here the increase of I_F with P should be associated with the increase of the dissociation ratio of the CF_4, and to the increase of the excitation efficiency of the F atoms. In addition, the reason of the higher I_F of the Ar/CF_4 than the O_2/CF_4 plasma should be related mainly to a higher excitation efficiency of the atomic F in the Ar/CF_4 plasma, because of the higher plasma density of the Ar/CF_4 gas mixture than the O_2/CF_4, as evidenced by the results in Fig. 1.

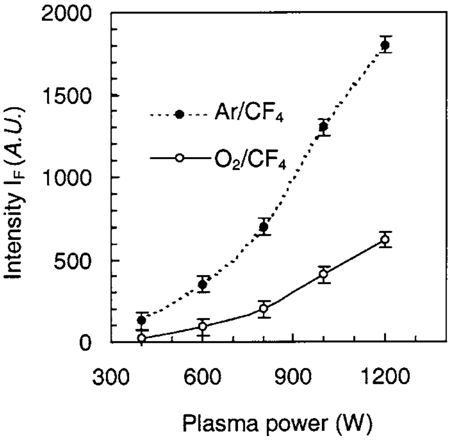

FIG. 4. Optical emission intensity of atomic F at the wavelength of 684.6 nm as a function of plasma power for the gas mixture of $Ar/CF_4=7/3$ or $O_2/CF_4=7/3$. The pressure was 10 mTorr, and the substrate was not biased.

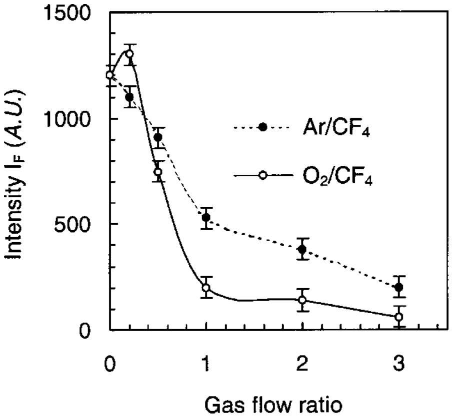

FIG. 5. Optical emission intensity of atomic F at the wavelength of 684.6 nm as functions of the gas flow ratios of Ar/CF_4 and O_2/CF_4. The plasma power was 600 W, pressure was 10 mTorr, and the substrate was not biased.

The dependencies of I_F on the Ar/CF_4 and O_2/CF_4 gas flow ratios are illustrated in Fig. 5. Here P was kept at 600 W, and gas pressure was 10 mTorr. It is seen in Fig. 5, I_F decreases all the way with the increase of Ar/CF_4 gas flow ratio; but for the O_2/CF_4 gas mixture, I_F exhibits an initial rise when the ratio increases to ~0.2, and then it drops down quickly with further increase of the O_2/CF_4 ratio. It is known that oxygen could react with CF_x radicals in the plasma, producing carbon oxides (CO, CO_2) and atomic F.[11,12] This could be the reason for the initial increase of the I_F. However, this effect was counterbalanced by further diluting effect of the O_2 addition, so that I_F dropped down at higher O_2/CF_4 ratio. The excitation efficiency of the F atoms should not change much with the variation of the gas ratio at the same plasma power, since the plasma density did not change much with the gas ratio at constant P, as evidence by the results in Fig. 2. Therefore, we can judge form Fig. 5, the concentration of atomic F was enormously diluted by increasing the Ar/CF_4 or O_2/CF_4 flow ratio to over 2/1, and at the same time, the concentration of other radicals (CF, CF_2, CF_3) dissociated from the CF_4 should be also greatly reduced when above dilution was made.

B. Etch rate and selectivity

To check the chemical etching effect of different processing gas or gas mixtures ($O_2, Ar, CF_4, Ar/CF_4, O_2/CF_4$), their etching rates to the As_2S_3 were tested without applying rf bias to the substrate for reducing the ion bombardment effect of the plasma. The results were list in Table I. The applied plasma power was 600 W, and pressure 10 mTorr for all the

TABLE I. Etch rate of As_2S_3 films floated in different plasma with a power of 600 W.

Sample	Gas flow (sccm)	Etch time (min)	Etch rate (nm/min)
1	O_2=70	10	0
2	Ar=70	10	20
3	CF_4=90	2	1500
4	CF_4/Ar=30/70	2	210
5	CF_4/O_2=30/70	2	130
6[a]	CF_4/O_2=30/70	2	20
7[b]	CF_4/O_2=30/70	2	100

[a]The sample surface was preoxidized in an O_2-plasma.
[b]The sample was positive biased with dc 60 V.

samples. The substrate was floated in the plasma with a floating potential of −5 to −10 V for samples 1–6. As seen from Table I, the etch rates are 0, 20, and ~1500 nm/min for pure O_2, Ar, and CF_4 plasma, respectively. This proves that the O_2 plasma has no chemical etching effect to the As_2S_3, but the CF_4 plasma has a very strong chemical etch to the As_2S_3. The etch rate by the CF_4 plasma was greatly reduced to 130 or 210 nm/min by feeding 70% Ar or O_2 gas, respectively, to the processing gas mixture, as demonstrated by the etch rates of samples 4 and 5 in the table.

It is reasonable for the pure O_2 plasma to have no chemical etch effect to the As_2S_3, since all the possible products (As_2O_3, SO_2, etc.) are not volatile at low temperature. In fact, the surface of the As_2S_3 could be oxidized after the O_2-plasma irradiation. As compared with sample 5 in Table I, the etch rate of sample 6 by CF_4/O_2 plasma reduced from 130 to 20 nm/min in the first 2 min after its surface was preirradiated using the O_2 plasma for 10 min. The etch rate of sample 6 was found to become normal (130 nm/min) again after the first 2-min-etching. This indicates that a more resistant layer to the CF_4 plasma was formed on the surface of the As_2S_3 film after the O_2 plasma irradiation. We believed that this layer was composed of the oxides of As_2O_3 and SO_2, because that the O_2 plasma is well known to be very effective to oxidize the surface of many solid materials, including GaAs,[13] Al,[14] and Si,[15] etc., and it is also know that the surfaces of solid As and S can even spontaneously oxidize in air.[16]

The low etch rate (20 nm/min) of pure Ar plasma for sample 2 in Table I was generated by a pure physical sputtering effect of the plasma. Ar is an inert gas, having no chemical etching effect, but Ar ions are much heavier than O ions, they can remove material via physical sputtering effect. Even though there was no rf power being applied to the substrate, there was still a total ion bombardment potential of ~35 V, contributed by a substrate floating potential of −10 V, and a plasma potential of +25 V. It was thus possible for the Ar ions to generate a physical sputtering effect to the As_2S_3 film, which is a low-density and soft solid material. In addition, Ar ion bombardment is well know to be able to enhance the surface chemical etching effect of many solid materials exposed in fluorine or fluoride gases.[17] This could be one of the reasons for a higher etch rate of the As_2S_3 by the Ar/CF_4 plasma than by the O_2/CF_4 plasma at the same gas ratio, as seen from the etch rates of samples 4 and 5 in Table I.

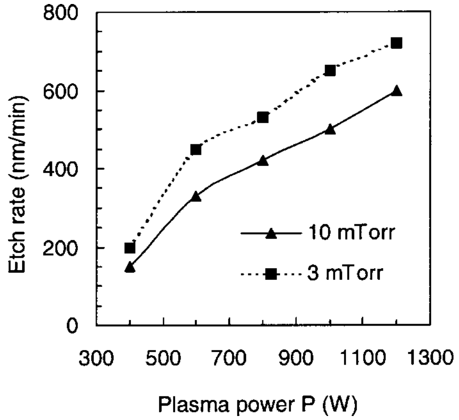

FIG. 6. Etch rate of the As_2S_3 films vs the helicon plasma power P, with O_2/CF_4=7/3, V_b=−100 V, and pressure 3 or 10 mTorr.

In addition, the possibility and degree of the chemical etch to the As_2S_3 induced by the neutral reactive species (F, CF, CF_2, CF_3) in the O_2/CF_4 plasma was also checked. We applied a positive dc bias of 60 V to the substrate to repel all the positive ions, and to attract only electrons coming from the plasma. A etch rate of ~100 nm/min was obtained in this case as seen in Table I for sample 7. This etch rate is only a little bit lower than that (130 nm/min) of sample 5 being etch with a total ion bombardment potential of ~30 V. This indicates that the chemical etch by the neutral species in the O_2/CF_4 plasma plays a major role for etching the As_2S_3. The chemical etch by the neutral species could be enhanced by ion and electron irradiation to the surface of the As_2S_3 as observed for the surface chemical etch of other materials in fluorine based gases.[17] The main etching products of the As_2S_3 in the CF_4 plasma could be arsenic fluorides (AsF_x) and sulfuric fluorides (SF_x), since they are known to be volatile at room temperature.

The dependence of the etch rate on the helicon plasma power P is displayed in Fig. 6. The applied substrate bias V_b was −100 V, O_2/CF_4=7/3, and pressure 3 or 10 mTorr. The etch rate is seen to increase significantly from ~200 to over 700 nm/min when increasing P from 400 to 1200 W as for the case of the gas pressure of 3 mTorr. The increase of the etch rate with P can be explained by the increase of the plasma density and the dissociation ratio of the CF_4 gas, as indicated by the results in Figs. 1 and 4. The increase of the etch rate when reducing the processing gas pressure from 10 to 3 mTorr was also related to the increase of the plasma density, as evidenced in Fig. 3.

The etch rates of the As_2S_3 as functions of the processing gas flow ratio of O_2/CF_4 and Ar/CF_4 are depicted in Fig. 7. The applied P was 600 W, bias V_b−100 V, and pressure 10 mTorr. As shown Fig. 7, the etch rate of the As_2S_3 is over 2000 nm/min with pure CF_4 plasma (at O_2/CF_4=0), but it decreases dramatically to a few hundred nm/min when in-

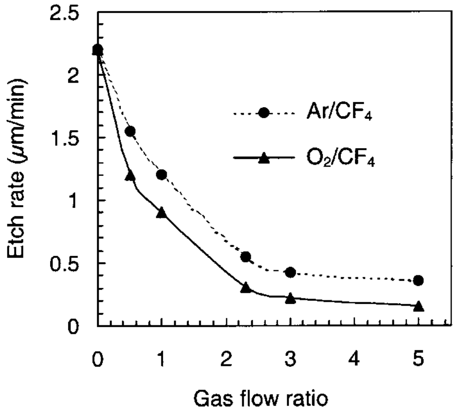

FIG. 7. Etch rate of As_2S_3 as functions of Ar/CF_4 and O_2/CF_4 gas flow ratios, with a plasma power 600 W, substrate bias −100 V, and pressure 10 mTorr.

creasing the Ar/CF_4 or O_2/CF_4 ratio to over 2/1; and a higher etch rate is generated using Ar/CF_4 than O_2/CF_4 gas mixture at the same gas ratio. These results can be explained by the plasma-diagnosing results shown in Figs. 2 and 5. As concluded from Fig. 5, when increasing the Ar/CF_4 or O_2/CF_4 ratio to over 2/1, the concentrations of the atomic F and other reactive species in the plasma decreased greatly, and thus the etch rates decreased dramatically. In addition, the ion current density of Ar/CF_4 plasma is always higher than that of the O_2/CF_4 plasma at the same gas ratio as showing in Fig. 2; and an Ar ion is much heavier than a O ion, making the Ar^+ has stronger bombardment effect than the O^+. The ion bombardment not only produces physical sputtering effect, but also enhances the chemical etching effect of neutral reactants. These are some of the reasons for the higher etch rate of the Ar/CF_4 than the O_2/CF_4 gas mixture at the same gas ratio.

The etch rates of the Al mask as functions of the processing gas flow ratios of CF_4/O_2 and CF_4/Ar are depicted in Fig. 8. The applied P was 600 W, V_b−100 V, and pressure 10 mTorr. As seen in Fig. 8, the etch rate of Al also decreases with the increase of the O_2/CF_4 or Ar/CF_4 gas flow ratio; and a much higher etch rate is generated using the Ar/CF_4 than the O_2/CF_4 gas mixture at the same gas ratio. In fact, Al is known to become oxidized quickly in air, especially in a O_2 plasma,[14,18] so that a dense Al oxide (Al_2O_3) layer of 3–5 nm thick normally forms on the Al surface to prevent further oxidation of the Al. The Al_2O_3 is also known to have very high resistance to the etch of the CF_4 plasma.[14] The addition of O_2 to CF_4 gas was, therefore, of benefit in improving the resistance of the Al masks to CF_4-plasma etching. Whereas, compared with the O_2 feeding, the Ar addition to CF_4 was in favor of intensifying the ion enhanced chemical etch and ion sputtering to the Al mask, leading to a quicker erosion of the Al mask.

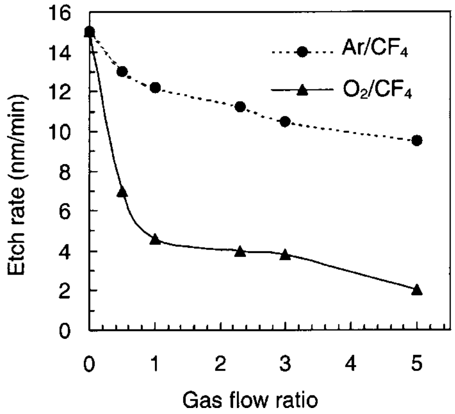

FIG. 8. Etch rate of Al mask layer as functions of Ar/CF_4 and O_2/CF_4 gas flow ratios, with plasma power 600 W, substrate bias −100 V, and pressure 10 mTorr.

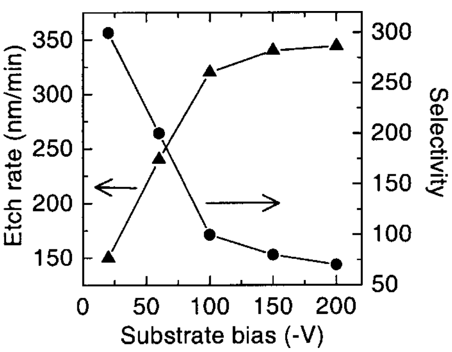

FIG. 9. Etch rate of As_2S_3 and the etching selectivity of As_2S_3/Al vs the substrate bias V_b with $O_2/CF_4=7/3$, $P=600$ W, and pressure 10 mTorr.

The etch rate of the As_2S_3 and its etching selectivity relative to the Al mask are depicted in Fig. 9 as functions of the substrate bias (V_b). The applied P was 600 W, processing gas ratio $O_2/CF_4=7/3$, and pressure ~10 mTorr. This figure shows that the As_2S_3 etch rate increases quickly with V_b when $-V_b < 100$ V, and then it becomes near saturated at higher bias. The increase of the etch rate with the bias is generally caused by the enhancement of ion bombardment effect.[19] Figure 9 also shows that the As_2S_3/Al etch selectivity deceases with V_b, but a very high As_2S_3/Al selectivity of ~80–100 is still obtained in the bias range of −100 to −150 V. This is very important for achieving vertical waveguide sidewalls, and for accurate control of the waveguide width.

C. Profile of the etched waveguides

Figure 10 illustrates the micrographs of the As_2S_3 waveguides etched under different O_2/CF_4 plasma conditions. The O_2/CF_4 gas flow ratio was found to be one of the main parameters influencing the amount of undercutting. A serious undercut of more than 1.0 μm could be generated for a 3 μm thick waveguide if pure CF_4 plasma was applied, and a strong undercut of ~0.8 μm for the 3 μm thick waveguide occurred even when the CF_4 was diluted with 50% O_2, as for the waveguide shown in Fig. 10(a), which was etched with $O_2/CF_4=1:1$, $P=600$ W, and $V_b=-120$ V. The degree of undercutting was reduced to ~0.12 μm when increasing the O_2/CF_4 ratio to 7:3 whilst keeping other plasma parameters constant, as for the waveguide shown in Fig. 10(d).

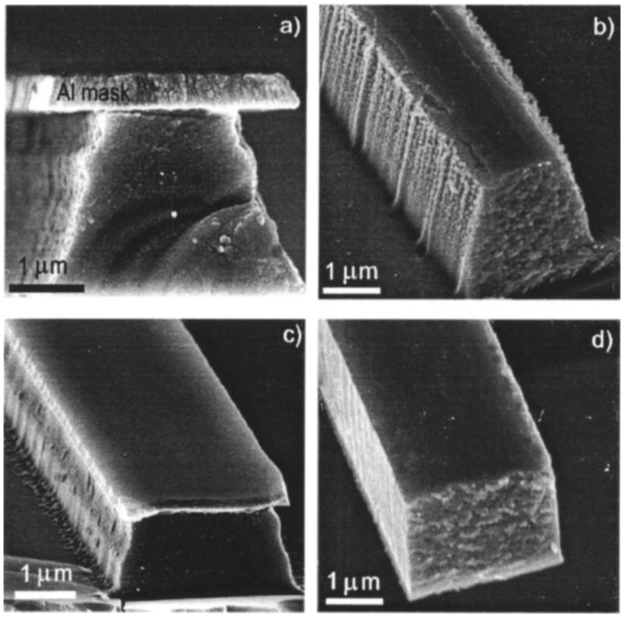

FIG. 10. Micrographs of the As_2S_3 waveguides obtained using different etching condition: (a) $O_2/CF_4=1/1$, $P=600$ W, and $V_b=-120$ V; (b) $O_2/CF_4=7/3$, $P=1000$ W, and $V_b=-120$ V; (c) $O_2/CF_4=7/3$, $P=600$ W, and $V_b=-50$ V; (d) $O_2/CF_4=7/3$, $P=600$ W, and $V_b=-120$ V. The processing pressure was 10 mTorr for all samples.

Another parameter affecting the etching anisotropy was the helicon plasma power P. The degree of undercutting was found to increase with P whilst keeping other plasma parameters constant, as illustrated in Fig. 10, where the sidewalls of the waveguides changed from near vertical [in Fig. 10(d)] to quite slanted [in Fig. 10(b)] when P was increased from 600 to 1000 W due to the undercutting effect.

The substrate bias also played an important role in determining the undercutting. As seen in Fig. 10, again holding other plasma parameters constant, the waveguide obtained using a low V_b of −50 V appeared to have a larger undercut of ~0.45 μm [in Fig. 10(c)], compared with the waveguide [in Fig. 10(d)] obtained using a high V_b of −120 V. The undercut resulting from low bias is commonly observed in plasma etching of different materials, and it is related to inadequate ion bombardment, and/or to insufficient control of the directions of the ions.[19]

To explain the undercut caused by the low O_2/CF_4 ratio or high plasma power, we need to consider the etching mechanisms. There are three basic plasma-etching mechanisms: physical sputtering, ion-enhanced chemical etching, and chemical etching.[19] The first 2 etching effects are directional, or anisotropic, and they will not cause undercutting if enough substrate bias is applied. The last etching effect, pure chemical etching induced by neutral reactants is an isotropic process, which is responsible for the undercutting. It has been proven by the results in Table I that neutral reactants in the O_2/CF_4 plasma play a major role in etching the As_2S_3. This is the reason for the strong undercut observed for some of the waveguides displayed in Fig. 10. Therefore, in order to reduce the undercutting, the isotropic etch effect induced by the neutral species need to be greatly weakened, while the anisotropy etch effects should be enhanced. This requires to reduce the concentration of the neutral reactants, and to enhance the ion bombardment. The latter requirement was achieved simply by increasing the substrate bias, while the former was achieved by the dilution of the CF_4 gas using O_2, and by the reduction of the plasma power, as demonstrated by the results shown in Fig. 10.

In fact, as seen in Figs. 4 and 5, the intensity of the F-line at 684.6 nm is actually very low (~100) under the plasma conditions of $P=600$ W and $O_2/CF_4=7/3$, compared with that (~700) obtained at a higher power of 1200 W, or with that (~1200) of the pure CF_4 plasma (at $O_2/CF_4=0$). Therefore the concentrations of the atomic F, as well as other neutral reactants, were relatively very low under the plasma conditions of $P=600$ W and $O_2/CF_4=7/3$. This greatly limited the isotropic etching effect of the plasma to the sidewalls of the waveguides. On the other hand, the ion current density was seen not to change much with the variation of the O_2/CF_4 ratio while holding other parameters constant, as evidence in Fig. 2. This allows the degree of ion bombardment not to change much when varying the O_2/CF_4 ratio. As a result, the isotropic chemical etch was greatly limited while a relative strong anisotropic etch or ion-bombardment enhanced chemical etch was remained when increasing the O_2/CF_4 ratio. Therefore, near vertical sidewalls of the waveguide [in Fig. 10(d)] were obtained with the optimized plasma conditions of $P=600$ W, $O_2/CF_4=7/3$, and $V_b=-120$ V.

There should be no polymer passivation layer formed on the sidewalls of the waveguides when using the CF_4/O_2 plasma to etch the As_2S_3, since the O_2 plasma is very effective to remove the polymer layer deposited from any carbon fluoride gases,[20] and the oxygen acts as scavenger of CF_x radicals, reducing the sources for the polymer formation. We have originally suspected that there could be an oxide layer formed on the sidewall of the waveguide, which might act as a passivation layer to inhibit the undercutting. However, this is proved to be unlikely. Although, an oxide layer can be generated on the As_2S_3 surface in a pure O_2 plasma as indicated by the etching behavior of sample 6 in Table I, the oxide layer could not form in the O_2/CF_4 plasma, as evidenced by the fact that a high etch rate of over 100 nm/min of the As_2S_3 was observed in the CF_4/O_2 plasma, even when the sample was floated or positive biased, as shown in Table I for samples 5 and 7. The etching process of the CF_4/O_2 plasma might suppress the oxide formation process even on the sidewall surfaces, where only little or even no ion bombardment was received.

The sidewall roughness of the As_2S_3 waveguides was found to mainly come from the side etching effect of the plasma, besides from the edge roughness of the original Al mask patterns. As shown in Fig. 10, very rough sidewalls were obtained as long as a big undercutting was present, as for those shown in Figs. 10(a)–10(c). Whereas, smooth sidewalls were obtained when the undercutting was greatly reduced as for the waveguide shown in Fig. 10(d). The sidewall roughness of the waveguides shown in Figs.

10(a)–10(c) was over ~150 nm, as determined using the FESEM, but it was below 50 nm for the waveguide shown in Fig. 10(d). Reducing the roughness of the sidewalls is very important for the waveguide fabrication, since a rough surface causes significant scattering loss from the waveguide.[21]

IV. SUMMARY

In summary, plasma etching to As_2S_3 thin films for waveguides fabrication in a helicon plasma reactor has been studied. The plasma etching behaviors and mechanisms were explained base on the etching results, and on the characteristics of the plasma diagnosed using Langmuir probe and optical spectroscopy techniques.

The O_2 plasma showed no chemical etching effect to the As_2S_3, but it could oxidize the surface of the As_2S_3. The Ar plasma had a strong sputtering effect to the As_2S_3. The CF_4 plasma exhibited a too strong chemical etch to the As_2S_3, and had to be diluted for reducing the undercutting and sidewall roughness of the waveguides. The neutral reactants in the CF_4 plasma play a major role in etching the As_2S_3, and their etching effect could be enhanced by ion bombardment.

Ar and O_2 gases were compared as the additives to dilute the CF_4 processing gas. The O_2 showed a better dilution effect than the Ar in reducing the etch rate of the As_2S_3, and an O_2/CF_4 plasma generated a much lower erosion rate to the Al masks than a Ar/CF_4 plasma at the same gas flow ratio. A very high As_2S_3/Al etching selectivity of ~80–100 was obtained using the O_2/CF_4 plasma even at a very high substrate bias of −100 to −150 V.

The dependence of the etch rate of the As_2S_3 on the gas flow ratio, plasma power and substrate bias were measured. It was found that the etch rate decreased dramatically from over 2000 nm/min to a few hundred nm/min when the gas flow ratio of the Ar/CF_4, or O_2/CF_4 was increased from 0 to over 2. The etch rate also shown to decrease significantly when reducing the plasma power or substrate bias.

Serious undercutting and very rough sidewall occurred when there was a strong isotropic etch, or insufficient substrate bias was applied. The isotropic etch process were greatly limited by reducing the concentrations of neutral reactants in the plasma through a heavy dilution of the CF_4 gas using O_2 addition, and through the reduction of the plasma power. As_2S_3 waveguides with near vertical and very smooth sidewalls were obtained using an optimized CF_4/O_2 plasma with a flow ratio of $O_2/CF_4=7/3$, plasma power 600 W, substrate bias −120 V, and processing gas pressure ~10 mTorr.

Although, some guidelines and understandings are present in this paper for the plasma etching of the As_2S_3 thin films, further studies are however still required to improve the etching results, and to clarify the etching chemistry.

ACKNOWLEDGMENTS

The supports of Australian Photonics Cooperative Research Centre, and of the Australian Research Council through its Federation Fellow (Barry Luther-Davies) and Centre of Excellence (CUDOS) programs are gratefully acknowledged.

[1] T. Cardinal, K. A. Richardson, H. Shim, A. Schulte, R. Beatty, K. Le Foulgoc, C. Meneghini, J. F. Viens, and A. Villeneuve, J. Non-Cryst. Solids **256**, 353 (1999).
[2] A. Saliminia, A. Villeneuve, T. V. Galstyan, S. Larochelle, and K. Richardson, J. Lightwave Technol. **17**, 837 (1999).
[3] C. B. Pedroso, E. Munin, A. B. Villaverde, J. A. Medeiros Neto, N. Aranha, and L. C. Barbosa, Opt. Eng. **38**, 214 (1999).
[4] C. C. Huang, D. W. Hewak, and J. V. Badding, Opt. Express **12**, 2501 (2004).
[5] J. F. Viens, C. Meneghini, A. Villeneuve, T. V. Galstian, E. J. Knystautas, M. A. Duguay, K. A. Richardson, and T. Cardinal, J. Lightwave Technol. **17**, 1184 (1999).
[6] S. Ramachandran and S. G. Bishop, Appl. Phys. Lett. **73**, 3196 (1998).
[7] S. Spalter, H. Y. Hwang, J. Zimmermann, G. Lenz, T. Katsufuji, S.-W. Cheong, and R. E. Slusher, Opt. Lett. **27**, 363 (2002).
[8] Y. L. Ruan, W. T. Li, R. Jarvis, N. Madsen, A. Rode, and B. Luther-Davies, Opt. Express **12**, 5140 (2004).
[9] A. V. Rode, A. Zakery, M. Samoc, R. B. Charters, E. G. Gamaly, and B. Luther-Davies, Appl. Surf. Sci. **97**, 481 (2002).
[10] A. J. Perry, D. Vender, and R. W. Boswel, J. Vac. Sci. Technol. B **9**, 310 (1991).
[11] R. Agostino, F. Cramarossa, S. Benedicts, and G. Ferraro, J. Appl. Phys. **52**, 1259 (1981).
[12] C. J. Mogab, A. C. Adams, and D. L. Flamm, J. Appl. Phys. **49**, 3796 (1978).
[13] C. R. Liu, and L. Liu, J. Phys. D **21**, 799 (1988).
[14] W. T. Li, D. A. P. Bulla, J. Love, and B. Luther-Davies, C. Charles, and R. Boswell, J. Vac. Sci. Technol. A **23**, 146 (2005).
[15] P. Hoffmann, R. P. Mikalo, and D. Schmeisser, J. Non-Cryst. Solids **303**, 6 (2002).
[16] P. Hari, C. Cheney, G. Luepke, S. Singh, N. Tolk, J. S. Sanghera, and I. D. Aggarwal, J. Non-Cryst. Solids **270**, 265 (2000).
[17] J. W. Coburn and H. F. Winters, J. Appl. Phys. **50**, 3189 (1979).
[18] A. Quade, H. Wulff, H. Steffen, T. M. Tun, and R. Hippler, Thin Solid Films **377–378**, 626 (2000).
[19] *Plasma Etching*, edited by D. M. Manos and S. L. Flamm (Academic, New York, 1989).
[20] K. Han, J. Kim, and W. H. Jang, J. Appl. Polym. Sci. **79**, 176 (2001).
[21] D. A. P. Bulla, W. T. Li, C. Charles, R. Boswell, A. Ankiewicz, and J. Love, Appl. Opt. **43**, 2978 (2004).